# Supplementary Information

## S1 Biological material

| Plasmids | | | |
|---|---|---|---|
| **Plasmid Name** | **Codes for** | **Function** | **Addgene** |
| UPG | AtUBQ10p::PCP-mGFP5 (hyg resistance in plants) | Ubiquitous expression of PCP-GFP fusion | |
| UPmCh | AtUBQ10p::PCP-mCherry (hyg resistance in plants) | Ubiquitous expression of PCP-mCherry fusion | |
| UMsfG | AtUBQ10p::MCP-sfGFP (hyg resistance in plants) | Ubiquitous expression of MCP-sfGFP fusion | |
| AL13Rb | PP7-Gus-Luc + AtUBQ10p::H2B-mScarlet (kan resistance in plants) | Promoterless PP7 reporter and red nuclear marker | |
| AL12R | AtUBQ10p::H2B-mScarlet + PP7-Gus-Luc (kan resistance in plants) | Promoterless PP7 reporter and Histone-mScarlet RFP nuclear marker | |
| AL13Rb-35S | 35S-PP7 reporter in AL13Rb | Reports on 35S promoter activity and labels nuclei | |
| AL13Rb-GAPC2 | GAPC2-PP7 reporter in AL13Rb | Reports on Arabidopsis GAPC2 promoter activity and labels nuclei | |
| AL12R-HSP70 | HSP70-PP7 reporter in AL12R | Reports on Arabidopsis HSP70 promoter activity and labels nuclei | |
| AL13Rb-HsfA2 | HsfA2-PP7 reporter in AL13Rb | Reports on Arabdiopsis HsfA2 promoter activity and labels nuclei | |
| AL12R-EF-Tu | EF-Tu-PP7 reporter in AL12R | Reports on Arabidopsis EF-Tu promoter activity and labels nuclei | |
| AL12R-HSP101 | HSP101-PP7 reporter in AL12R | Reports on Arabdiopsis HSP101 promoter activity and labels nuclei | |
| UtB2N7 | AtUBQ10p::tagBFP2-NLS | nuclear localized blue fluorescent protein marker | |
| UBC1cer60G | AtUBC1::60mer-mGFP5 | Weak ubiquitous expression of an ER-targeted 60mer monomer fused to mGFP5 | |
| UBC1cer120G | AtUBC1::mGFP5-60mer-mGFP5 | Weak ubiquitous expression of an ER-targeted 60mer monomer fused to two mGFP5 | |

**Table S1**

| Arabidopsis lines generated in this study | | |
|---|---|---|
| **Name** | **Transgenes (refer to the 'Plasmids' table)** | **Usage** |
| UPG-6 | UPG | For transformation with reporter constructs |
| UPG-9 | UPG | For transformation with reporter constructs |
| AL13Rb-35S | UPG and AL13Rb-35S | Image 35S promoter activity in Figure 1 |
| AL12R-HSP101-1 | UPG and AL12R-HSP101 | Image AtHSP101 promoter activity in Figures 2 to 5 |
| AL13Rb-HSP101-2 | UPG and AL13Rb-HSP101 | Image AtHSP101 promoter activity in Figure 5 |
| AL13Rb-HsfA2-1 | UPG and AL13Rb-HsfA2 | Image AtHsfA2 promoter activity in Figures 3 and 4 |
| AL13Rb-HsfA2-2 | UPG and AL13Rb-HsfA2 | Image AtHsfA2 promoter activity in Figure 5 |
| AL12R-EF-Tu-1 | UPG and AL12R-EF-Tu | Image AtEF-Tu promoter activity in Figures 3, 4 and Fig. S4 |

**Table S2**

| Arabidopsis Gene Identifiers | | |
|---|---|---|
| **Gene abbreviation** | **Gene name** | **AGI** |
| UBQ10 | Polyubiquitin 10 | AT4G05320.2 |
| H2B | Histone 2B | AT5G22880.1 |
| GAPC2 | Glyceraldehyde-3-phosphate dehydrogenase C2 | AT1G13440.1 |
| HSP70 | Heat shock protein 70 | AT3G12580.1 |
| UBC1 | Ubiquitin carrier protein 1 | AT1G14400.1 |
| HSP101 | Heat shock protein 101 | AT1G74310.1 |
| HsfA2 | Heat shock transcription factor A2 | AT2G26150.1 |
| EF-Tu | GTP binding Elongation factor Tu family protein | AT1G07920.1 |

**Table S3**

## S2 Calculations

### S2 .1 Decomposition of total variability into extrinsic and intrinsic noise

In this section we derive the formulas for the total, intrinsic and extrinsic noise ($\eta^2_{tot}$, $\eta^2_{int}$, and $\eta^2_{ext}$, respectively) based on the two-reporter approach developed by ***Elowitz et al.*** (***2002***). As noted by ***Hilfinger and Paulsson*** (***2011***) and explained at length by ***Fu and Pachter*** (***2016***), these expressions stem from the law of total variance, which states that, for a random output variable $A$ and a random input variable $X$, the total variance of $A$ can be decomposed as the sum

$$\underbrace{\mathrm{Var}(A)}_{\text{total variance}} = \underbrace{\mathrm{Var}_X(\langle A|X\rangle_A)}_{\text{explained variance}} + \underbrace{\langle \mathrm{Var}_A(A|X)\rangle_X}_{\text{unexplained variance}}, \tag{S1}$$

where the subscripts $X$ or $A$ indicate that the average or the variance is taken over different values of $X$ or $A$, respectively.

Applied to the problem of gene expression variability, $A$ represents the expression level of the gene of interest and $X$ corresponds to the cellular state indicating, for example, the concentration in each given cell of all molecules that affect the expression of that gene such as RNAP. The first term on the right-hand side of Equation S1 is referred to as the *explained variance* and captures how much the average value of $A$ varies across different values of $X$. The second term is referred to as the *unexplained variance* and captures how much the expression of $A$ varies in cells that share the same value of $X$.

Because the identity and values of $X$ are typically not known and/or not experimentally accessible, ***Elowitz et al.*** (***2002***) devised a two-reporter system to determine the explained and unexplained components of the total normalized variance, which they termed extrinsic ($\eta^2_{ext}$) and intrinsic ($\eta^2_{int}$) noise, respectively. In this approach, each cell has two identical but distinguishable alleles of the gene of interest. In their statistical model, these two alleles are identical in all respects meaning that their distribution over cells and over time are the same. For the purpose of this derivation, let us call $A_i$ and $B_i$ the expression level of each allele in the $i$-th cell and normalize $A$ and $B$ to their means such that

$$\frac{A_i}{\langle A\rangle} = 1 + \delta A_i, \tag{S2}$$

where $\delta A_i$ is the fractional deviation of the expression level $A_i$ from the mean $\langle A\rangle$. Similarly, for B we normalize to

$$\frac{B_i}{\langle B\rangle} = 1 + \delta B_i. \tag{S3}$$

In the following calculations we will make use of the measurable quantities $\delta A_i$ and $\delta B_i$ to eliminate the unknown quantity $X$ from Equation S1. We start by deriving an expression for $\eta^2_{ext}$ defined here as the explained component of the total variance of the normalized $\delta A$ distribution

$$\eta^2_{ext} = \mathrm{Var}_X(\langle \delta A_i|X\rangle_A). \tag{S4}$$

Note that, since $X$ is a random variable, so is $\langle \delta A_i|X\rangle_A$, and we can write its variance as

$$\eta^2_{ext} = \langle\langle \delta A_i|X\rangle^2_A\rangle_X - \langle\langle \delta A_i|X\rangle_A\rangle^2_X. \tag{S5}$$

Because both alleles are identical, $\langle \delta A_i|X\rangle_A$ is equal to $\langle \delta B_i|X\rangle_B$, which allows us to write Equation S5 as

$$\eta^2_{ext} = \langle\langle \delta A_i|X\rangle_A\langle \delta B_i|X\rangle_B\rangle_X - \langle\langle \delta A_i|X\rangle_A\rangle_X\langle\langle \delta B_i|X\rangle_B\rangle_X. \tag{S6}$$

Note that, in this model, the variability in the values of $A_i$ and $B_i$ for cells with the same $X$ are independent of each other since we assume that they are not explained by $X$. Because of this independence, $\langle A_i\rangle\langle B_i\rangle = \langle A_iB_i\rangle$ for a given $X$. Applied to the first term in Equation S6, the extrinsic noise can be written as

$$\eta^2_{ext} = \langle\langle \delta A_i\delta B_i|X\rangle_{A,B}\rangle_X - \langle\langle \delta A_i|X\rangle_A\rangle_X\langle\langle \delta B_i|X\rangle_B\rangle_X. \tag{S7}$$

We now note that the double angle brackets in the first term in the right-hand side of Equation S7 call for averaging the value of $\delta A_i\delta B_i$ in cells with the same $X$ and then averaging again over all possible values of $X$. Similarly, the second term in the equation calls for averaging over $A_i$ or $B_i$ for a given $X$, and then averaging over $X$. This allows us to eliminate $X$ in the equation and simplify our expression to

$$\eta^2_{ext} = \langle \delta A\delta B\rangle - \langle \delta A\rangle\langle \delta B\rangle, \tag{S8}$$

which is the definition of covariance. Thus,

$$\eta^2_{ext} = \mathrm{Cov}(\delta A, \delta B). \tag{S9}$$

This makes intuitive sense, as the model assumes that, since $A$ and $B$ are identical genes that respond to $X$ in the exact same way, the variance in the expression of $A$ that is explained by $X$ is identical to the variance in the expression of $B$ that is explained by $X$. As a result, the extrinsic noise measures how $A$ and $B$ coordinately vary across cells.

We now turn our attention to the derivation of the intrinsic noise, which we define as the unexplained component of the variance in the normalized $A$ distribution, namely

$$\eta_{int}^2 = \langle \mathrm{Var}_A(\delta A_i | X) \rangle_X. \tag{S10}$$

Replacing the unexplained variance in Equation S1 with $\eta_{int}^2$, the explained variance by its formulation as extrinsic noise from Equation S9, and rearranging leads to

$$\eta_{int}^2 = \mathrm{Var}(\delta A_i) - \mathrm{Cov}(\delta A_i, \delta B_i). \tag{S11}$$

Because this equation does not involve $X$ we don't need the subscripts anymore: all variances are calculated across values of $\delta A$ and $\delta B$. We now note that the total variance of $\delta A$ and $\delta B$ must be the same since they have the same distribution over cells and over time. Therefore we are allowed to express the first term in the right-hand side of Equation S11 as the average variance of the $\delta A_i$ and $\delta B_i$ distributions

$$\eta_{int}^2 = \frac{1}{2}\left[\mathrm{Var}(\delta A_i) + \mathrm{Var}(\delta B_i)\right] - \mathrm{Cov}(\delta A_i, \delta B_i). \tag{S12}$$

Rearranging Equation S12 leads to

$$\eta_{int}^2 = \frac{1}{2}\left[\mathrm{Var}(\delta A) + \mathrm{Var}(\delta B) - 2\mathrm{Cov}(\delta A, \delta B)\right]. \tag{S13}$$

Now, using the identity stating that the variance of a sum is the sum of the variances minus their covariance, Equation S13 becomes

$$\eta_{int}^2 = \frac{1}{2}\mathrm{Var}(\delta A_i - \delta B_i). \tag{S14}$$

Finally, we define the total noise $\eta_{tot}^2$ as the total variance of the normalized $\delta A_i$ distribution. As noted before, because the distributions of $\delta A_i$ and $\delta B_i$ are identical, so are their variances. Therefore, the total noise can be calculated from the average

$$\eta_{tot}^2 = \frac{1}{2}\left[\mathrm{Var}(\delta A_i) + \mathrm{Var}(\delta B_i)\right], \tag{S15}$$

which satisfies

$$\eta_{tot}^2 = \eta_{ext}^2 + \eta_{int}^2. \tag{S16}$$

Note that, here, we considered $\delta A$ loosely as the "expression level" of gene $A$. This analysis can be applied to any metric of gene expression such as the instantaneous transcription rate, or the total amount of produced mRNA.

### S2 .2 Determining transgene copy number by qPCR

In this section, we present our calculation for determining the number of transgene insertions from the $\Delta CT$ values resulting from qPCR taking the amplification efficiency into account. Given a starting number of DNA molecules $N_0$, the total number of molecules after $C$ amplification cycles is given by

$$N(C) = N_0(2\epsilon)^C, \tag{S17}$$

where $\epsilon$ corresponds to the amplification efficiency, or the fraction of molecules that are duplicated in each cycle. The number of amplification cycles $CT$ that takes to amplify the number of DNA molecules from $N_0$ to $N_{ct}$ can be described by

$$CT = \log_{2\epsilon}\left(\frac{N_{ct}}{N_0}\right). \tag{S18}$$

Changing the logarithm base and rearranging leads to

$$CT = \frac{\log_2\left(\frac{N_{ct}}{N_0}\right)}{1+\log_2(E)}. \tag{S19}$$

We now define an amplification efficiency constant $K$ as

$$K = \frac{1}{1+\log_2(E)}. \tag{S20}$$

Equation S19 then becomes

$$CT = K\log_2\left(\frac{N_{ct}}{N_0}\right). \tag{S21}$$

To experimentally obtain $K$ (and therefore $\epsilon$), we perform qPCR on serial dilutions of template DNA, thus varying $N_0$. We then plot $CT$ as a function of the $\log_2$ of the template concentration in order to obtain $K$ from the slope (Fig. S9A,B). We used genomic DNA from a transgenic Arabidopsis plant to perform this amplification on the PP7 transgene as well as on an internal control genomic sequence. We measured both PCR reactions to have an efficiency of $K = 1$ within experimental error. As a result, we can determine the ratio between the initial number of transgene molecules $N_0^t$ and the initial number of internal control molecules $N_0^c$ by calculating the $\Delta CT$

$$\Delta CT = CT^t - CT^c = K\log_2\left(\frac{N_{ct}}{N_0^t}\right) - K\log_2\left(\frac{N_{ct}}{N_0^c}\right) = \frac{N_0^c}{N_0^t} \tag{S22}$$

If the transgene occurs in a single insertion locus containing a single transgene copy per insertion, then in a T1 individual

$$\frac{N_0^c}{N_0^t} = 0.5, \tag{S23}$$

which corresponds to a $\Delta CT$ value of -1. Using this approach we were able to identify transgenic Arabidopsis individuals with a single insertion locus containing a single transgene insertion (Fig. S9C).

## S3 Supplementary Figures

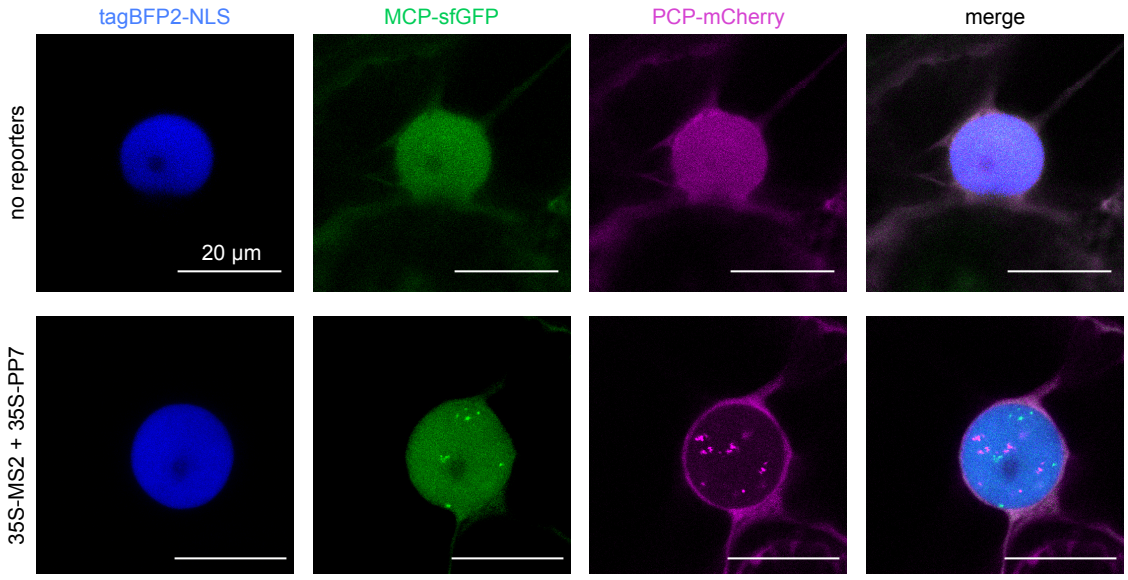


**Figure S1. Related to Figure 1F. MCP-sfGFP and PCP-mCherry are homogeneously distributed in the nucleus in the absence of transcription.** Maximum fluorescence projection snapshot of the nucleus of a Tobacco cell expressing MCP-sfGFP, PCP-mCherry and nuclear localized tagBFP2. No nuclear puncta appear in the absence of PP7 and MS2 reporters.

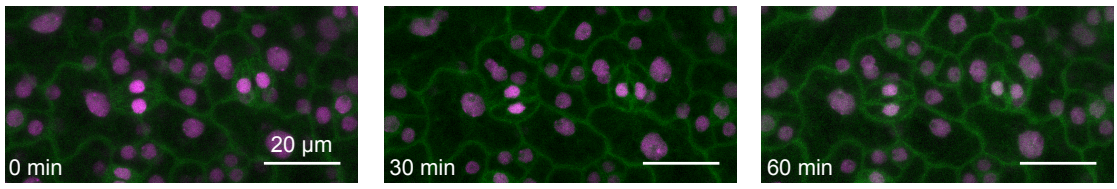


**Figure S2. Related to Figure 2A. Lack of HSP101 induction at room temperature.** Maximum z-projected image snapshots of the PCP-GFP/HSP101-PP7 Arabidopsis line imaged at room temperature. No spots were detected after continuous imaging for 80 minutes. Scale bar = 20 $\mu$m.

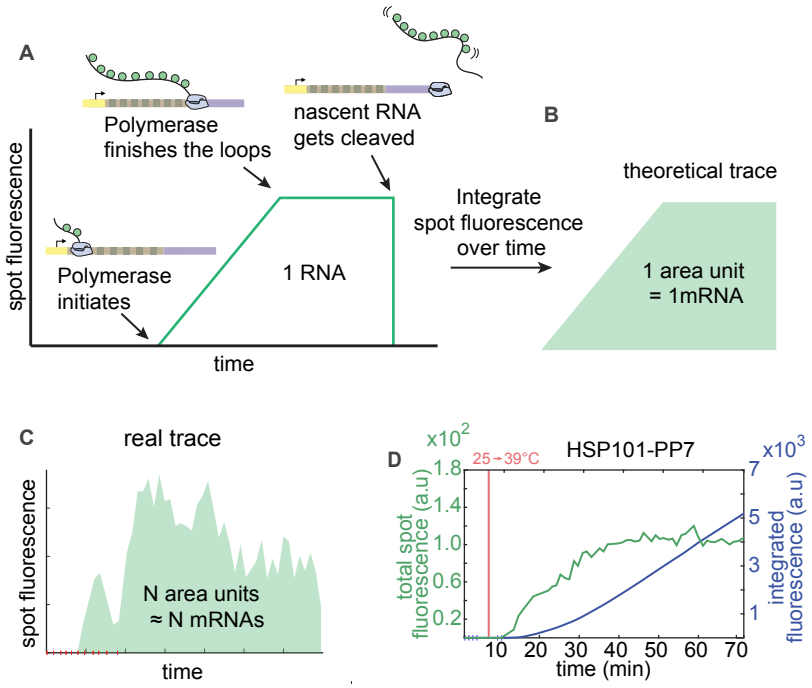


**Figure S3. Related to Figure 2B. Integrated fluorescence as a metric for total mRNA produced.** (A) Fluorescence profile of a single RNAP molecule as it traverses the gene. (B) Integrating this curve over time yields a unit of area associated with the production of a single mRNA molecule. (C) In the case of an actual transcription spot—resulting from the activity of multiple polymerase molecules—the integrated fluorescence over time will correspond to a number of area units equal to the number of produced mRNA molecules. **(D)** Data from a HSP101-PP7 replicate from Figure 2. Total spot fluorescence normalized by the number of cells in the field of view (green) and time integral of this signal (blue). The red horizontal line indicates when the stage temperature was shifted from room temperature to 39 °C.

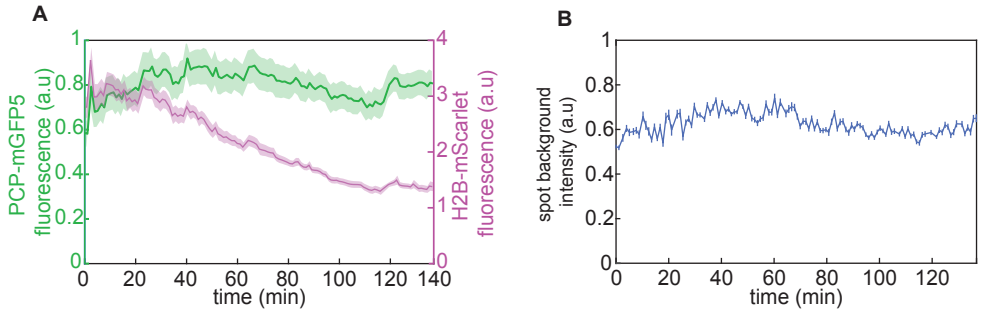


**Figure S4. Related to Figure 2B. Control for photobleaching (A)** Mean and standard error of nuclear fluorescence from PCP-GFP and Histone 2B-mScarlet in an Arabidopsis line expressing PCP-GFP and a reporter construct driven by the constitutive EF-Tu promoter imaged using our standard imaging conditions. There is no significant bleaching of the PCP-GFP signal even after imaging for more than two hours. However, there is evident bleaching of mScarlet. **(B)** No bleaching is observed in the fitted PCP-GFP spot fluorescence background in the same experiment either.

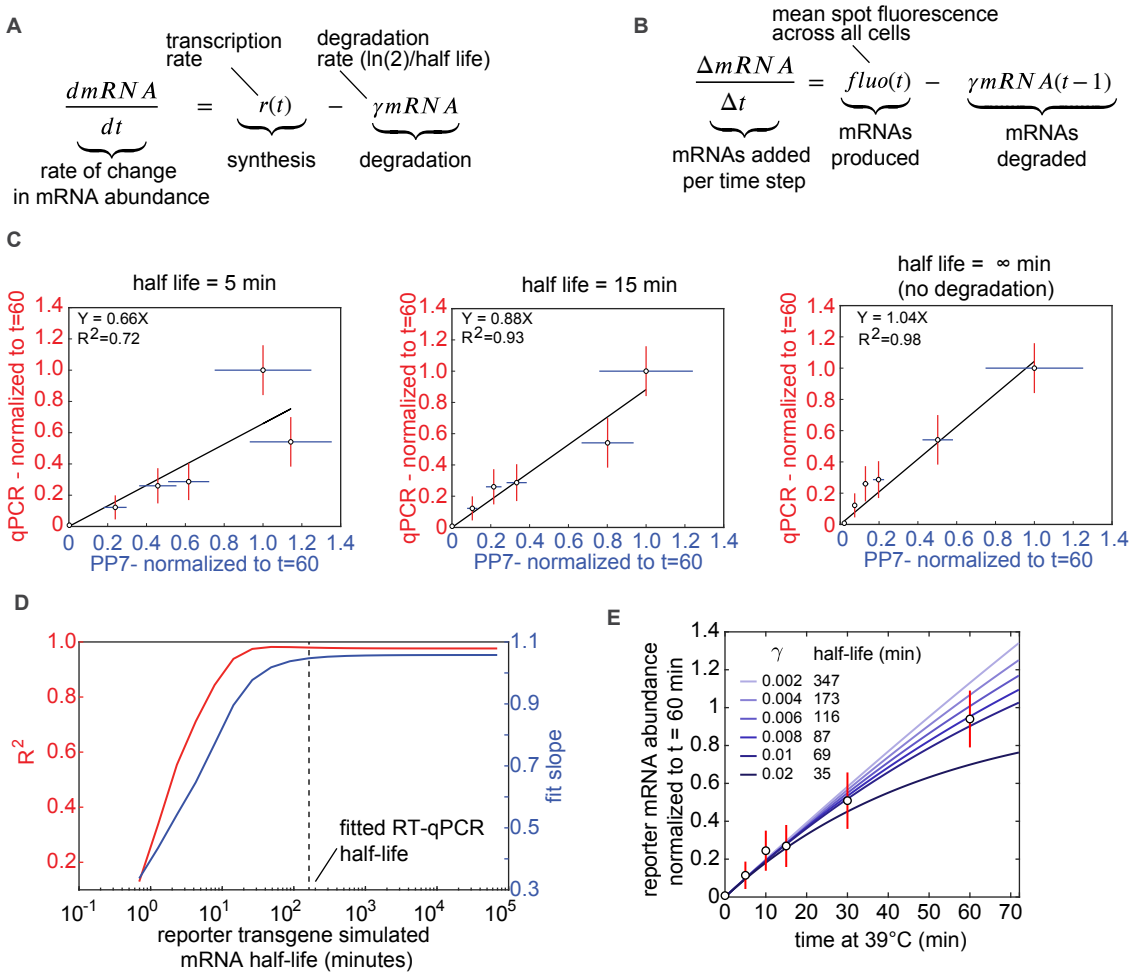


**Figure S5. Related to Figure 2B. Exploring the effect of the mRNA degradation rate on the validation of the PP7 system against RT-qPCR measurements. (A)** The rate of change in mRNA abundance is determined by a time-dependent rate of mRNA synthesis $r(t)$ and a constant mRNA degradation rate $\gamma$. **(B)** Discretized version of equation (A) used to obtain the accumulated mRNA based on spot fluorescence measurements. At each time point the rate of synthesis is equal to the spot fluorescence while the number of mRNA molecules accumulated up to the previous time point are degraded at a simulated rate $\gamma$. Note that the mRNA half-life is defined as $\tau_{1/2} = \ln(2)/\gamma$. **(C)** Linear regression between the reporter mRNA abundance measured by RT-qPCR versus microscopy as in Figure 2C using the equation in (B) to incorporate mRNA degradation into the microscopy-based measurement. Because microscopy only reports on the synthesized, and not the degraded mRNA, we considered different, constant degradation rates and included this correction in the linear regression. **(D)** Fit parameters ($R^2$ and fit slope) as shown in (C) were calculated for a range of mRNA degradation rates expressed as half-lives. There is a good correlation and a constant slope between RT-qPCR and microscopy for half-lives longer that ~10 minutes. The dashed horizontal line indicates the fitted reporter mRNA half-life obtained in (C). **(E)** the reporter mRNA abundance measured by RT-qPCR was fitted to the mRNA accumulation model in (A) assuming a constant synthesis rate. mRNA accumulation according to RT-qPCR is almost linear on the timescales tested, resulting in a relatively long half-life. This half-life value is within the regime where there is a good correlation between PP7 fluorescence and qPCR (see vertical dashed line in (D)).

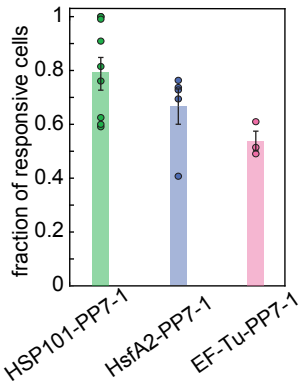


**Figure S6. Related to Figure 3A. Reproducibility of the fraction of responsive cells.** Mean and standard error of the fraction of transcriptionally responsive cells, defined as the number of nuclei that display reporter activity at least at one time point during the experiment divided by the total number of nuclei in the field of view (see Fig. 3A, bars on the right of each heat map). Circles represent at least three biological replicates

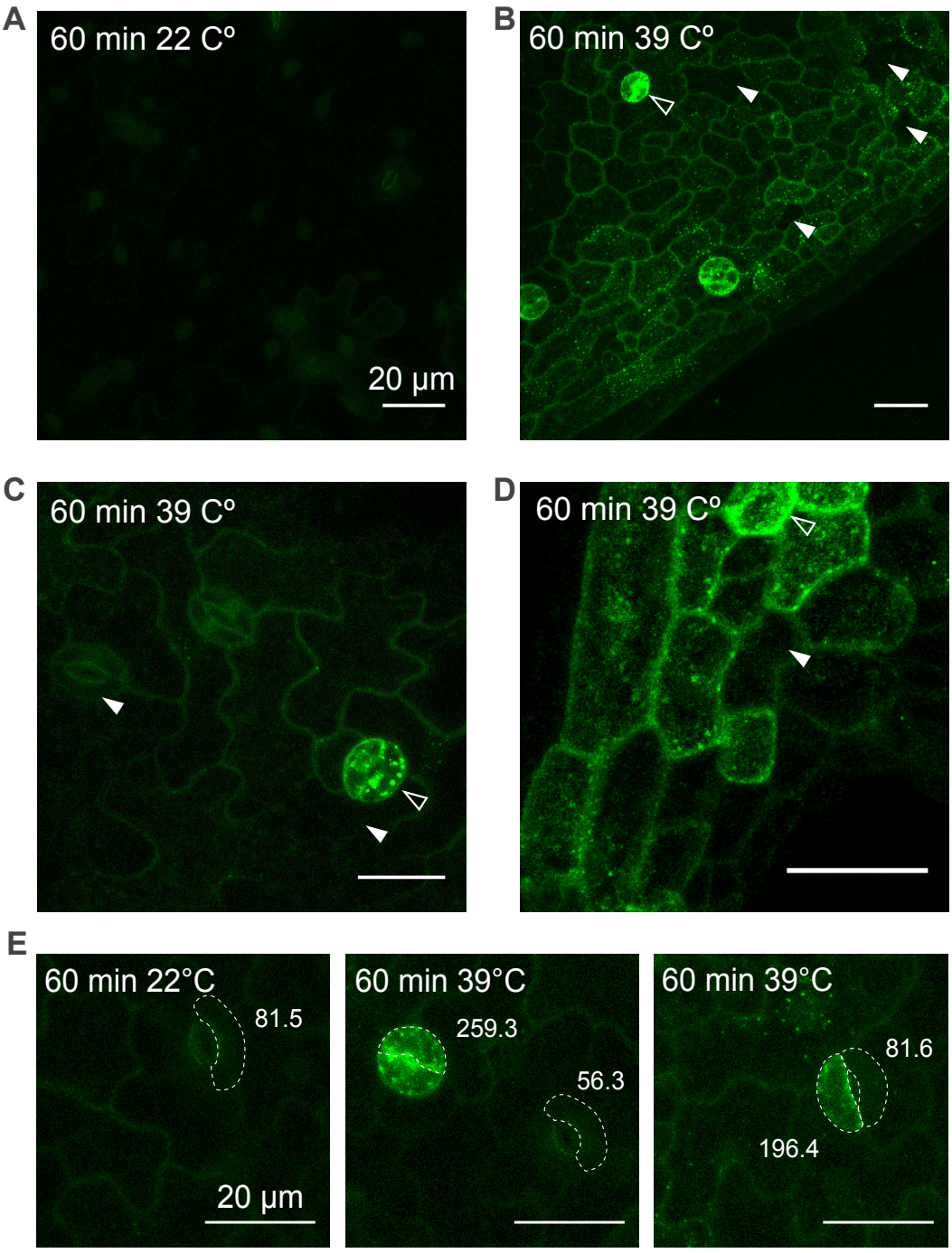


**Figure S7. Related to Figure 3: A rescue construct of HSP101-GFP reveals how refractory cells lead to substantial cell-to-cell heterogeneity in HSP101-GFP accumulation upon heat shock. (A-E)** Maximum fluorescence projections of leaf epidermis cells from *hsp101* knockout mutant plants complemented with a transgene coding for a HSP101-GFP fusion driven by 734 bp of the endogenous HSP101 promoter (***McLoughlin et al., 2016***). Detached leaves were treated with 39 or 22 °C for 60 minutes prior to imaging. **(A)** Untreated control. **(B-D)** Treated samples. White filled arrowheads indicate cells with negligible levels of GFP accumulation. Empty white arrowheads indicate cells with high levels of GFP accumulation. **(E)** Quantification of GFP fluorescence in treated and untreated cells. The dashed line highlights cells whose fluorescence was calculated. The numbers next to each cell correspond to the integrated GFP fluorescence of the volume of each cell highlighted.

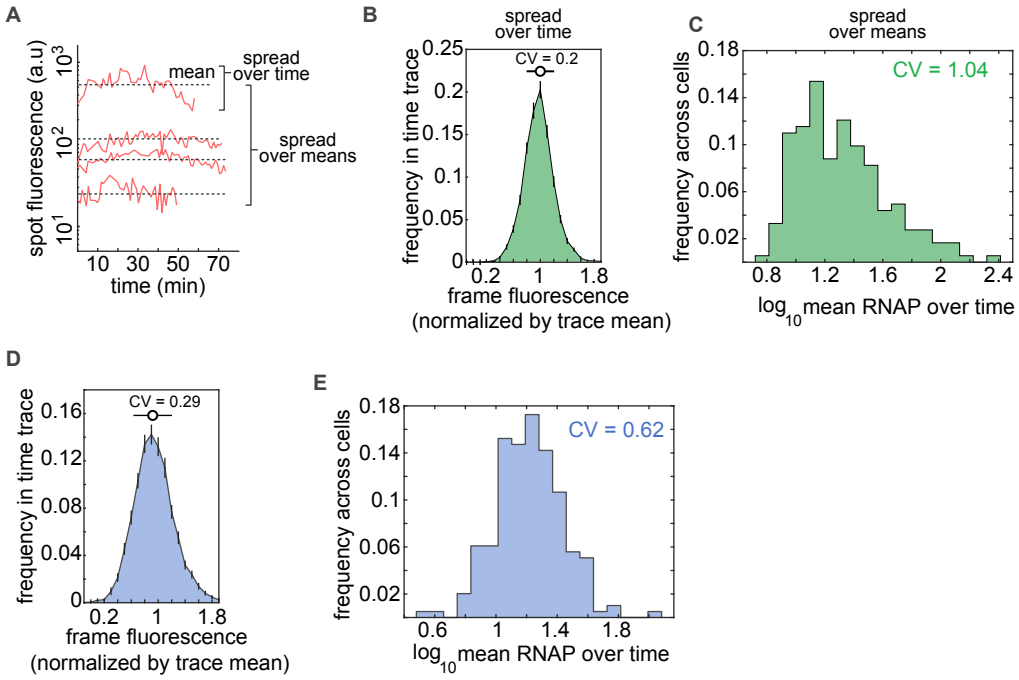


**Figure S8. Related to Figure 4: Spot fluorescence varies widely across cells but is relatively stable over time in individual cells. (A)** Representative spot fluorescence time traces in HSP101-PP7-1 replicates from Figure 3. Dashed lines correspond to the mean level of fluorescence of each trace over time. The spread of fluorescence values around this mean for each individual trace ("spread over time") informs about temporal fluctuations in transcriptional activity for each individual spot (B). The variability of mean fluorescence values across cells, is captured by the "spread over means", and informs about cell-to-cell heterogeneity in activity (C). **(B)** Distribution of frame fluorescence values normalized by the mean over time for each fluorescence trace pooled from all HSP101-PP7-1 replicates from Figure 3. The spread over time of fluorescence values of a given spot is very close to the mean, resulting in a coefficient of variation (CV=standard deviation/mean) of 0.2. **(C)** Distribution of mean fluorescence over time (see dashed lines in (A)) of all cells in HSP101-PP7-1 replicates. The average transcriptional activity varies widely across cells, with a coefficient of variation of 1.04. **(D,E)** Same as (B) and (C) for HsfA2-PP7-1 fluorescence traces pooled across replicates from Figure 4.

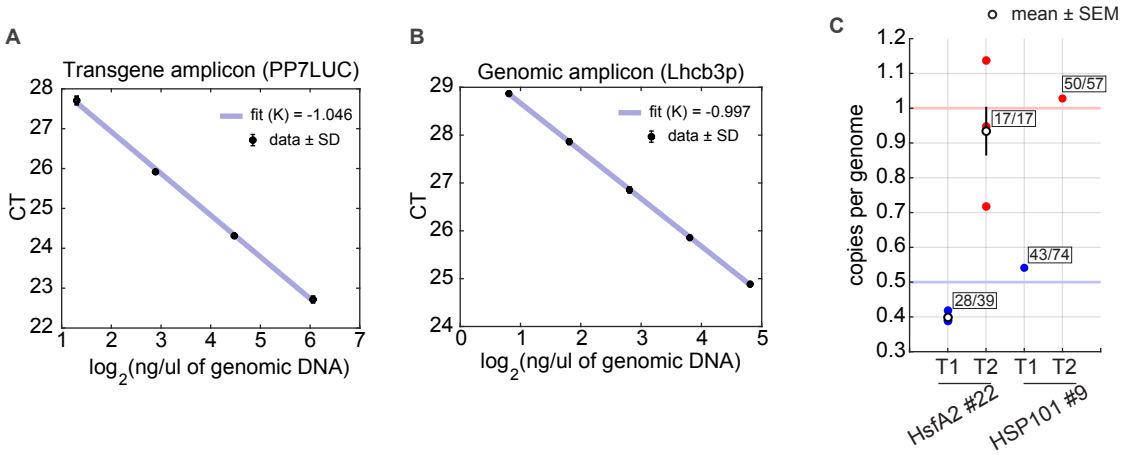


**Figure S9. Amplification efficiency of primer pairs and determination of the copy number of single insertion lines. (A)** qPCR results for serial dilutions of transgenic Arabidopsis plants using primer pairs targeting the reporter transgene. **(B)** Same as (A) for a primer pair targeting a genomic location upstream of the *Lhcb3* gene. In (A) and (B), the slope of the linear fit corresponds to $K = 1/(1 + log_2(\epsilon))$ where $\epsilon$ is the amplification efficiency. **(C)** Number of copies of the PP7 reporter transgene per genome copy in two single insertion reporter lines in the T1 and T2 generations. The horizontal blue line indicates the expected value for a single-copy hemizygous plant where the insertion locus contains a single copy of the transgene. The red horizontal line indicates the expected value for a plant homozygous for a single insertion where this insertion contains a single copy of the transgene. The ratios next to each data point indicate the fraction of survivors over the total number of plated seeds under kanamycin selection.

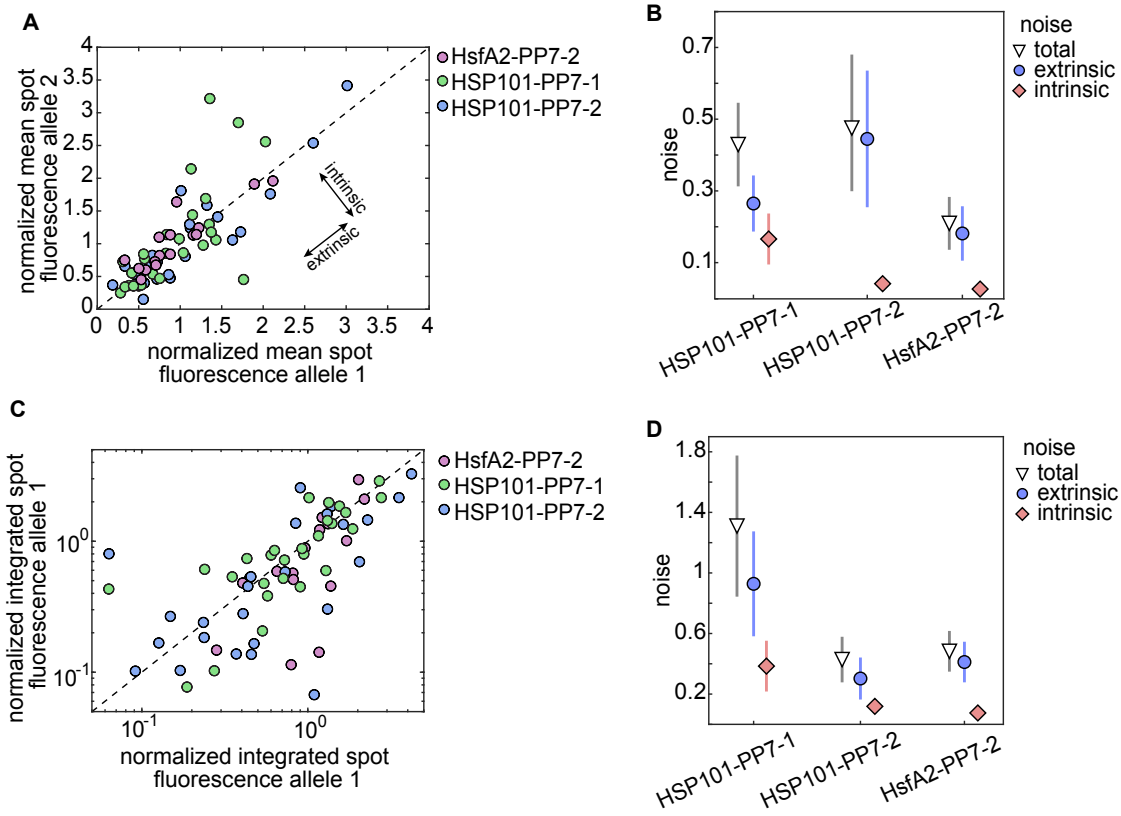


**Figure S10. Related to Figure 5 Extrinsic noise is larger than intrinsic noise among nuclei with two active alleles. (A)** Scatter plot showing the mean spot fluorescence over time for allele pairs belonging to the same nucleus in three different single-insertion lines homozygous for the PP7 reporter. **(B)** Decomposition of the total variability in (A) into its intrinsic and extrinsic components. **(C)** Scatter plot of integrated fluorescence over time in allele pairs belonging to the same nucleus in three different single-insertion reporter lines homozygous for the PP7 transgene (same as Figure 5E except that inactive alleles are not included). **(C)** Decomposition of the total noise in (C). In (A) and (C) values were normalized to the mean across all alleles in that line and the diagonal line shows y=x. Error bars in (B) and (C) correspond to the bootstrapped error.

## S4 Supplementary Videos

S1. **Video 1. Constitutive reporter in tobacco.** Movie of tobacco cell expressing PCP-GFP and GAPC2-PP7. The scale bar is 10 $\mu$m.

**Video 2. Inducible reporter in tobacco.** Movie of tobacco cell expressing PCP-GFP and HSP70-PP7 under heat shock treatment starting at 10 min. The scale bar is 10 $\mu$m.

**Video 3. Inducible HSP101-PP7 reporter in Arabidopsis tissue.** Movie of leaf cells in Arabidopsis line stably transformed with PCP-GFP and HSP101-PP7 under heat shock treatment starting at 6 min. The scale bar is 10 $\mu$m.

**Video 4. Inducible HsfA2-PP7 reporter in Arabidopsis tissue.** Movie of leaf cells in Arabidopsis line stably transformed with PCP-GFP and HsfA2-PP7 under heat shock treatment starting at 8 min. The scale bar is 10 $\mu$m.

**Video 5. Constitutive reporter in Arabidopsis tissue.** Movie of leaf cells in Arabidopsis line stably transformed with PCP-GFP and EF-Tu-PP7. The scale bar is 10 $\mu$m.

**Video 6. Arabidopsis plant homozygous for an inducible reporter.** Movie of leaf cells in a homozygous Arabidopsis line stably transformed with PCP-GFP and HSP101-PP7 under a heat shock treatment starting at 0 min. The scale bar is 10 $\mu$m.